Image Correlation-Based Method to Assess Ciliary Beat Frequency in Human Airway Organoids

Woo June Choi, Jung-Ki Yoon, Bjorn Paulson, Chang-Hoon Lee, Jae-Joon Yim, Jong-Il Kim, and Jun Ki Kim, *Member, IEEE*

***Abstract*— Ciliary movements within the human airway are essential for maintaining a clean lung environment. Motile cilia have a characteristic ciliary beat frequency (CBF). However, CBF measurement with current video microscopic techniques can be error-prone due to the use of the single-point Fourier transformation, which is often biased for ciliary measurements. Herein, we describe a new video microscopy technique that harnesses a metric of motion-contrast imaging and image correlation for CBF analysis. It can provide objective and selective CBF measurements for individual motile cilia and generate CBF maps for the imaged area. The measurement performance of our methodology was validated with *in vitro* human airway organoid models that simulated an actual human airway epithelium. The CBF determined for the region of interest (ROI) was equal to that obtained with manual counting. The signal redundancy problem of conventional methods was not observed. Moreover, the obtained CBF measurements were robust to optical focal shifts, and exhibited spatial heterogeneity and temperature dependence. This technique can be used to evaluate ciliary movement in respiratory tracts and determine whether it is non-synchronous or aperiodic in patients. Therefore, our observations suggest that the proposed method can be clinically adapted as a screening tool to diagnose ciliopathies.**

***Index Terms*— Ciliary beat frequency, ciliary motion, human airway organoid, image correlation, motion-contrast imaging.**

Manuscript received June 29, 2021; revised September 9, 2021; accepted September 12, 2021. Date of publication September 15, 2021; date of current version February 2, 2022. This work was supported in part by the Basic Science Research Program under Grant 2019R1A2C2084122, Grant 2020R1F1A1072912, Grant 2020R1A6A1A03047972, and Grant 2020R1F1A1074033; in part by the Engineering Research Center (ERC) under Grant 2020R1A5A1018052; in part by the Medical Research Center (MRC) under Grant 2018R1A5A2020732; in part by the Brain Pool Program of the National Research Foundation (NRF) of Korea through the Ministry of Science and ICT under Grant 2020H1D3A1A02081127; in part by the Korean Ministry of Trade, Industry and Energy through the Industrial Technology Innovation Program under Grant 20000843; and in part by Korea Health Industry Development Institute through the Ministry of Health and Welfare, Republic of Korea, under Grant HI18C2391. *(Woo June Choi and Jung-Ki Yoon contributed equally to this work.) (Corresponding author: Jun Ki Kim.)*

Woo June Choi is with the School of Electrical and Electronics Engineering, Chung-Ang University, Seoul 06974, Republic of Korea.

Jung-Ki Yoon and Jae-Joon Yim are with the Division of Pulmonary and Critical Care Medicine, Department of Internal Medicine, Seoul National University College of Medicine, Seoul 03080, Republic of Korea.

Bjorn Paulson is with Asan Medical Center, Asan Institute for Life Science, Seoul 05505, Republic of Korea.

Chang-Hoon Lee is with the Division of Pulmonary and Critical Care Medicine, Department of Internal Medicine, Seoul National University Hospital, Seoul 03080, Republic of Korea.

Jong-Il Kim is with the Medical Research Center, Genomic Medicine Institute (GMI), Seoul National University, Seoul 03080, Republic of Korea.

Jun Ki Kim is with Asan Medical Center, Asan Institute for Life Science, Seoul 05505, Republic of Korea, and also with the Department of Convergence Medicine, University of Ulsan College of Medicine, Seoul 05505, Republic of Korea (e-mail: kim@seoul.amc.kr).

This article has supplementary downloadable material available at https://doi.org/10.1109/TMI.2021.3112992, provided by the authors.

Digital Object Identifier 10.1109/TMI.2021.3112992

I. Introduction

MOTILE cilia are microtubule-based hair-like organelles that line the apical surface of epithelial cells in lung airways, brain ventricles, and the oviduct, where ciliary movement driven by dynein protein activation mediates the transport of particles, cells, and fluids [1]–[3]. The multi-ciliated cells act as an essential physical barrier for the lung. Each cilium has a cyclic motion of fast stroke and slow recovery stroke movement. The ciliary array in the respiratory tract are not completely separated but synchronized movements with phase shift making larger waves. This metachronal waves push the mucus layer above the ciliary epithelium outwards. Thus, the inhaled foreign materials like dirt, chemicals, and pathogens which are trapped in mucus can be removed, resulting in mucociliary clearance [4], [5]. Defective cilia can occur in ciliopathies [6], which are inherited genetic disorders such as primary ciliary dyskinesia (PCD) [7], [8]. Additionally, constitutive damage to epithelial cells in chronic inflammatory diseases such as chronic obstructive pulmonary disease (COPD) [9] can also result in abnormal ciliary movement. Subsequently, defective or reduced ciliary motility can result in recurrent pneumonia leading to progressive destruction of lung architecture [10]. Therefore, modeling and quantifying the motion of respiratory cilia is generally used for exploring the pathophysiology of lung diseases.

One of the basic parameters used to evaluate ciliary function (e.g., beating in coordinated waves) is the ciliary beat frequency (CBF) [11]. Previously, the CBF has been measured by directly counting ciliary beats during visual inspection of a camera video file [12], [13], which was highly accurate but extremely time-consuming and unsuitable for real-time

analysis. Other methods using photodetectors [14], [15] have provided fast estimation of beat frequency by analyzing changes in the light intensity passing through the beating cilia. However, it was challenging for point-detection methods to visualize CBFs over the ciliated area. Of the current techniques, high-speed digital video microscopy [16]–[18] is routinely used to measure the CBF. Here, a digital camera sequentially captures bright-field microscopic ciliary images at 85–500 frames per second (fps). Subsequently, a spectral analysis of the time-course signal intensities at each pixel of the video by fast Fourier transformation (FFT) yields the frequency of light intensity fluctuation, which represents ciliary cycles. The FFT method is considered the modern gold standard for CBF estimation. However, this conventional method has some major issues. First, signal redundancy can occur either due to multiple ciliary organelle layers on epithelial cell edges or neighboring cilia. Other cells in motion may interfere with individual cilium trajectories, which distorts the intensity of the recorded signals in the trace. Consequently, the FFT result exhibits strong multiple harmonics that can lead to confounding and erroneous CBF interpretation. Second, although the user measures non-overlapping areas to avoid the signal redundancy, selection bias can occur. This is because cilia are poorly visible in the typical microscopy image due to relatively lower reflectivity than the surrounding tissue. These problems may hinder objective CBF assessments that could be critical to diagnose ciliopathies (e.g., cell-to-cell variability of CBFs has been observed for individual PCD patients [19]). Therefore, alternatives to the existing approach are desirable for acquiring reliable CBF measurements. Recent advancements in CBF measurements have been made using sophisticated microscopic techniques such as differential dynamic microscopy (DDM) [20], Doppler optical coherence tomography (OCT) [21], and micro-OCT (μOCT) [22]. DDM relies on two-dimensional (2-D) power spectrum analysis of difference images to retrieve information about dynamics in a sample (motile cilia), providing robust and automated CBF estimation [20]. Doppler OCT is an extension of OCT, an interferometry-based imaging modality to visualize internal structures of live sample with resolution of a few microns. This OCT technology has been used to quantify the cilia motion, in which CBF was estimated by measuring time-varying phase shifts in the OCT signals induced by ciliary movement during stroke cycles [21]. Furthermore, cilia imaging of the ultrahigh-resolution (<1 μm) μOCT has directly delineated the ciliary stroke patterns, allowing for the CBF assessment of individual cells [22]. Despite the promising results, however, these techniques might be not free of the redundancy issue.

Organoids are three-dimensional (3-D) cell aggregates derived from either adult or embryonic stem cells, capable of offering self-renewal, self-organization, and exhibiting organ functionality [23], [24]. With these unique features, the miniaturized organ-like cells act as authentic disease models in comparison to cell lines [24]. Organoids replicate human lung biology, and drug screening can be readily performed. They have been actively engineered to study early lung development, pathogenesis of genetic disorders and chronic lung diseases, and cell-based therapies [25]–[27]. Furthermore, using CRISPR/Cas9 genome editing technology, one can introduce or rescue genetic mutations in organoids, which enables the generation of long-term culture models for genetic disorders [28], [29]. However, depending on the target site and design of the CRISPR/Cas9 system [30], [31], genome editing efficiency varies as does the frequency of off-target events. As a result, genome editing can generate lung airway organoid models with different ciliary movements. Therefore, for understanding lung biology and pathology with organoids and CRISPR/Cas-9, it is important to assess cilia dynamics using a wide region of interest (ROI).

Here, we developed a novel assay to assess collective ciliary dynamics without signal redundancy, and successfully utilized this method in lung airway organoids with ciliated cells. To estimate CBF, the technique harnesses a video analysis which considers the cross-correlation between high-speed optical microscope images. In this study, the proposed method accurately assessed ciliary beating by calculating CBFs. Our image correlation strategy is robust to focal shifts and is an improvement over existing CBF estimation methods via FFT analysis. The method enabled the generation of a whole-organoid CBF map, and we evaluated whether CBF is temperature dependent. To our knowledge, this has not been previously achieved in airway organoid models. Finally, the method was tested to measure CBFs of partially defective cilia in genetic disorder organoid models developed with CRISPR/Cas9.

II. Materials and Methods

A. Human Airway Organoids

Human airway epithelial cells were collected by bronchoscopic brushing on the normal bronchus from patients during bronchoscopy. The airway organoids were established with the previously reported organoid culture [26], and followed by an air-liquid interface culture (Fig. 1A). The detailed protocol with modifications is provided in the Supplementary materials.[1] Collection and use of human specimens were reviewed and approved by the institutional review board of Seoul National University Hospital [1602-108-742].

B. Genome Editing of Organoids

Organoids with C-terminal truncation of Dynein Axonemal Assembly Factor 4 (DAAF4) were established by lentiviral transfection of SpCas9 and a guide RNA, according to the established protocol [32]. Sanger sequencing was performed to confirm the edited sequences. Details about materials and sequences are listed in the Supplementary materials.[1]

C. Imaging Setup

A home-built bright-field optical microscope was used (Fig. 1B). A 150 W halogen lamp (OSL2, Thorlabs, NJ, USA) was coupled with a Köhler illumination setup for lighting. Light rays ($\lambda_0 = 600$ nm) were directed onto an organoid sample via a non-polarized beam splitter (BS)

[1]Supplementary materials are available in the supporting documents/multimedia tab.

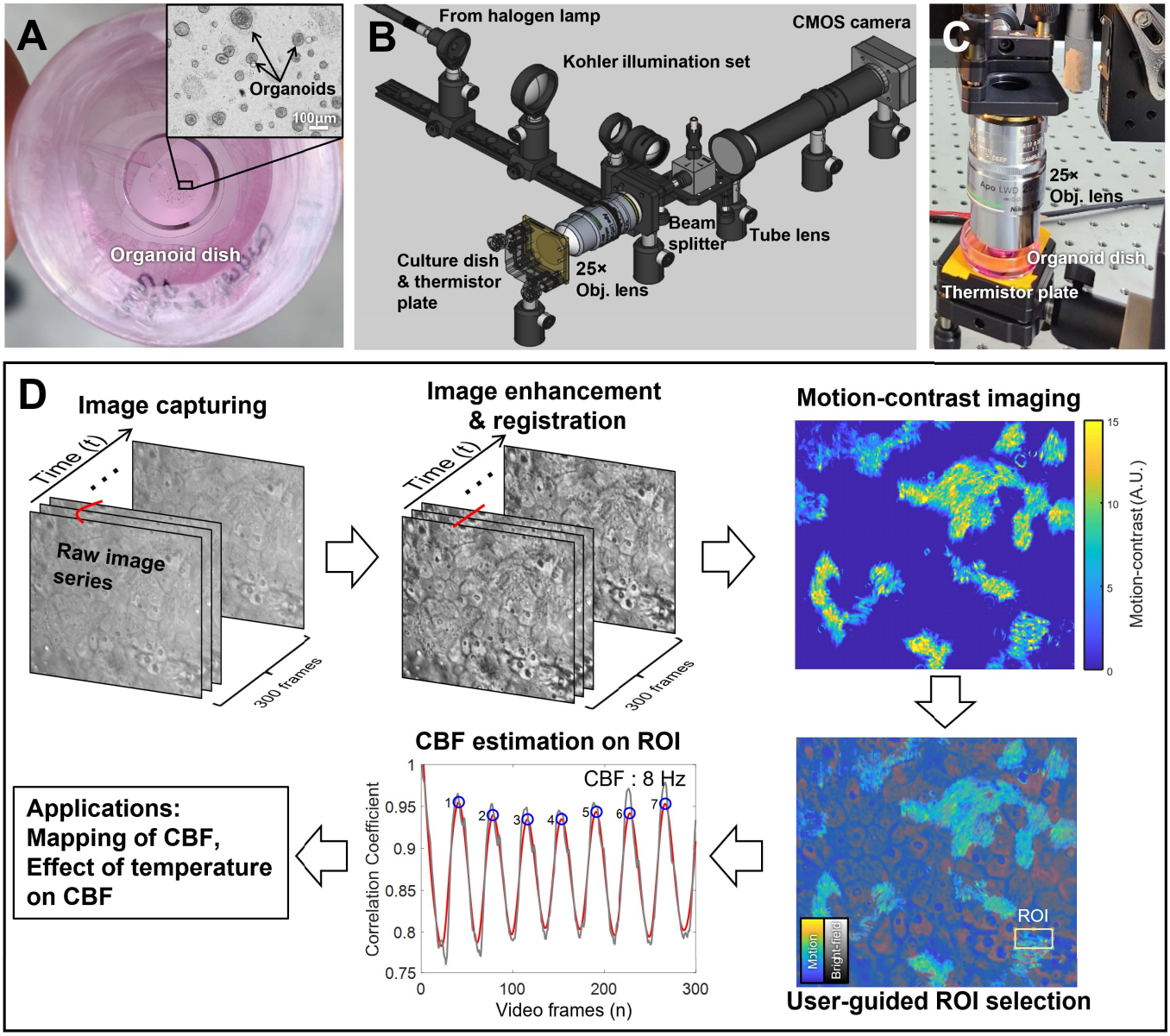

Fig. 1. Image correlation-based digital video microscopy allows CBF measurement of the motile cilia on human epithelial organoids. (A) Petri dish with cultured human airway organoids (inset) centered in the dish. (B) Schematic of a home-built reflectance microscope system. (C) Thermostatically controlled sample stage. (D) Flow chart illustrating CBF estimation procedure. First, a CMOS camera acquires images of an organoid in culture sequentially at 300 frames per second (fps). Second, contrast in the captured images is enhanced, and images are registered to correct mechanical motion artifacts. Third, a motion-contrast image depicting the motile cilia locations is generated with the image set. Fourth, considering the motion-contrast and the bright-field image, an ROI is selected for CBF analysis. Finally, the local peaks of a correlation coefficient waveform obtained from cross-correlation between the first and other frames were counted, and CBF for the ROI was calculated.

and a 25× water dipping objective lens (N25X-APO-MP, 1.1 N.A., 2.0 mm W.D., Nikon, Tokyo, Japan) (Fig. 1C). Light reflected from the sample was collected via the objective and the BS, and focused through a 0.75× infinity-corrected tube lens (f = 200 mm) onto a high-speed CMOS camera (VC-2MC-M340, 337.6 fps for free-run mode, 5.5 μm^2 pixel size, Viewworks, Seoul, Korea) capturing 8-bit gray-scaled images (2048 pixels × 1088 pixels) at 200 to 300 fps over a medium configuration Camera Link connection. With system magnification of 18.75×, system resolution was measured from the microscope image of a USAF 1951 resolution target (R3L3S1P, Thorlabs, NJ, USA) captured by our set-up, where the smallest patterns (group 7, element 6) on the resolution target were clearly resolved (not shown here). Therefore, the system resolution is estimated to be less than 4.3 μm. During recording, the temperature of the organoid culture was controlled by a closed-loop thermistor plate (TLK-H, Thorlabs, NJ, USA).

D. Image Correlation Analysis for CBF Measurement

The entire procedure for CBF measurement is illustrated in Fig. 1D. The captured images were contrast-enhanced in batches to improve viewing and then registered. Image

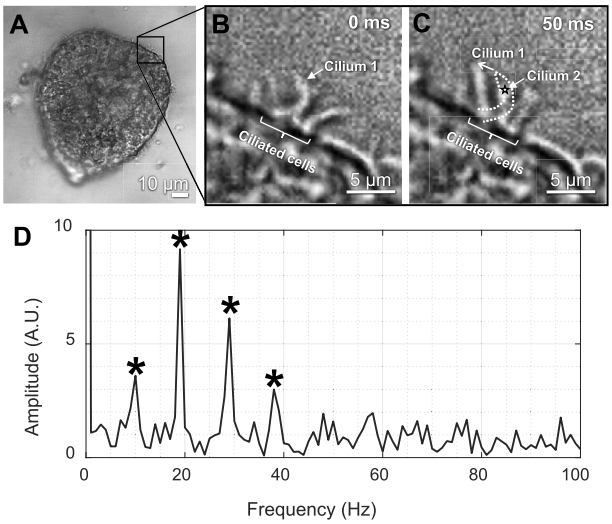

Fig. 2. Signal redundancy issue of conventional single-point fast Fourier transformation (FFT) method in CBF measurement. (A) Bright-field image of a healthy human airway organoid. (B) Magnification of the boxed area in (A), which shows a group of collective ciliated cells. (C) The same area as in (B), captured 50 ms later. (D) FFT spectrum of a time-course intensity profile recorded at 200 Hz for 1 s at the position (star) depicted in (C). Here, ciliary beat frequencies were confounded by harmonics (asterisks).

registration was performed with a function custom-written in MATLAB, by which each image was automatically aligned with a reference image (the first frame) by estimating the geometric translation transformation. Therefore, possible slow drift and mechanical motion artifacts in the recording that might interfere with ciliary motion signals were pre-corrected. To identify the cilia in the image, Eigen-decomposition (ED) filtering [33] was applied to the registered images. ED filtering is an adaptive clutter rejection technique that utilizes statistical properties of time-varying signals and effectively extracts signal dynamics (sourced from ciliary motion here) from the static background [33]. Thus, ED filtering generated a motion-contrast image, which improved localization of the cilia in the organoids. The motion-contrast image was observed, and a ROI involving the individual cilia was selected. Further, cross-correlation was performed with the ROI images, and we measured the similarity between the first frame (a reference frame) and the rest of the frames to determine the oscillatory correlation coefficients. Smoothing was taken to the correlation coefficients using a low-order polynomial fitting to remove possible spurious spikes on the profile. The peaks of the resulting coefficient waveform were counted, and the counts were divided by the recording period (total frames/frame rates), which represented the CBF for the cilia in the ROI. All procedures except for the user selection of ROI were fully automated in our CBF analysis software, written in MATLAB (Supplementary Video 1). However, the measurable range of CBF depends mainly on the sampling rate (frame rate) of the camera. According to the Nyquist theorem, the sampling rate should be at least two times greater (5–10 times in practice) than the ciliary beat frequencies to fully restore the temporal beating signals. Considering the maximum camera frame rate (∼337 fps) and the signal smoothing, therefore, we expect the maximum detectable CBFs with the current set-up to be less than 30 Hz.

E. Statistical Analysis

The data were statistically analyzed using a paired t-test, which was performed using Origin software (OriginLab, Northampton, MA, USA). A p-value of 0.05 was considered as the statistical significance threshold.

III. Results

A. Signal Redundancy Exhibited by CBF Measurement

We performed an analysis to determine whether the proposed methodology can handle signal redundancy better than the conventional method. Here, the CBFs in motile cilia were determined with the proposed method and the single-point FFT analysis technique, which were then compared. Two hundred images of human airway organoids (Fig. 2A) were captured at 200 fps, such that moving cilia aligned in the plane of focus were resolved. For instance, enlarged views of the boxed area in Fig. 2A captured at 0 and 50 ms are shown in Fig. 2B and 2C, respectively, showing that the tip of "cilium 1" at 0 ms moved leftward 50 ms later, whereas the neighboring "cilium 2" crossed the trace of "cilium 1". In the conventional method, a single point (star in Fig. 2C) was selected, and the pixel intensities over time were processed into an amplitude spectrum by FFT. The result (Fig. 2D) exhibited significant multiple spectral peaks (asterisks) due to interference from the movement of other cilia. Further, it was difficult for the users to determine the fundamental frequency of ciliary motion, which was estimated to be 9 Hz after manual counting by two physicians.

B. Assessment of Background Interference Effect

An image-based correlation technique was developed, and the same image stack used in Fig. 2 was analyzed with this technique. The bright-field image acquired from the box in Fig. 3A (same as Fig. 2A) was superimposed with a color-coded motion-contrast image (Fig. 3B), where yellow in color indicates high motility of cilia. Considering ciliated cells within the ROI (yellow box in Fig. 3B), the correlation between the ROI frames was calculated (Fig. 3C), which was followed by data smoothing (red line in Fig. 3C). The peaks of the coefficient waveform were counted (blue circles), and CBF was computed to be 9 Hz, which was consistent with the manual assessment. Note that if the correlation signal at the last frame is more than the mean of all peaks, it was considered a peak and counted. This indicated that the proposed approach as performed is better than other single-point-based FFT approaches in analyzing the movement of ciliated cells *in vitro*.

C. Assessment of Focal Shift Effect

Cilia are often captured out of focus because they are slender, micrometer-sized, and unevenly lined in the light-translucent organoid as well as *in vivo*; therefore, it is

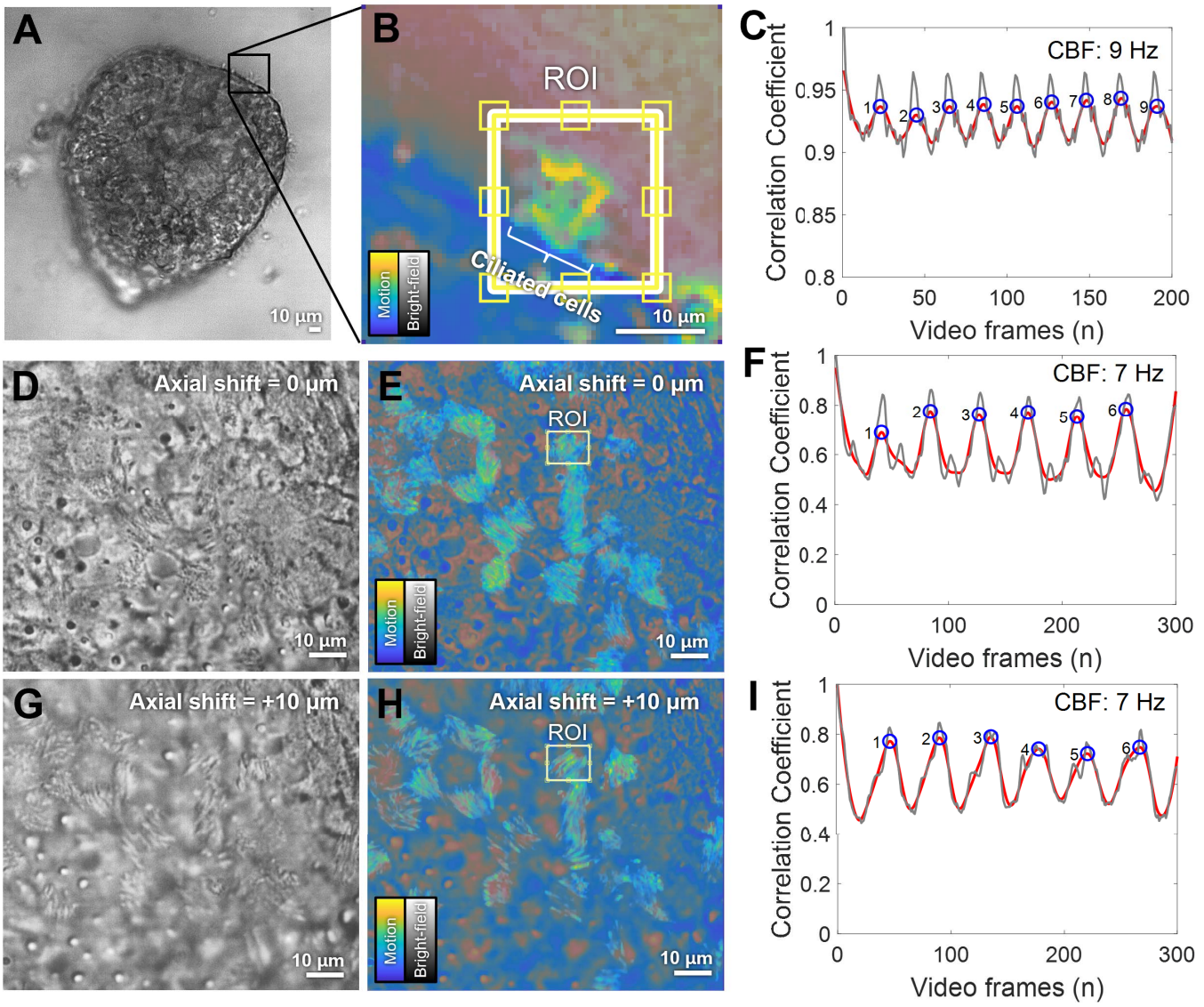

Fig. 3. Evaluation of the proposed CBF method. (A) Bright-field image, same as Fig. 2A. (B) The same magnification as Fig. 2B overlaid with a pseudo-colored motion-contrast image. An ROI for correlation calculation was manually selected (yellow box). (C) The correlation profile calculated from the region. The CBF calculated with counts of the peaks in the smoothed profile (red line) over 1 s (200 frames/200 fps) was consistent with the manual CBF grading of 9 Hz. (D-I) Sensitivity of the measurement by focal shift was assessed. (D) Image at original focus, where the background cellular substrate was in focus. (G) Image with shifted focus (+10 μm), where the background is blurred. (E, H) Motion-contrast images with equivalent ROIs and the effect of a focal shift. (F, I) Inter-frame correlation waveforms obtained from ROIs, showing focus-independent estimates of CBF (7 Hz).

not easy for users to adjust cilia to be within the focal plane. To assess the sensitivity of the method at different optical foci, cilia image stacks were collected twice from the same organoid. One stack contained focused and non-overlapping cilia in the organoid (Fig. 3D), and the other contained out-of-focus cilia collected with focus on an area that was 10 μm higher (Fig. 3G). Correlation was performed on identical ROIs (yellow boxes in Figs. 3E and 3H) and followed by smoothing. Here, the coefficient profiles (Figures 3F and 3I) differed significantly in the amount of noise; however, the resultant beat frequency estimate was identical in both cases. Interestingly, the unfocused image correlations appeared less noisy and matched the smoothed curves precisely (Fig. 3I). This demonstrated that our method is robust to focal shifts and can process out-of-focus images.

D. Spatial CBF Mapping

The proposed method was iterated over multiple ROIs in image stacks of an organoid. For example, the method was repeated for individual cilia (yellow boxes in Figure 4B) separately arranged in an organoid (#1 in Figure 4A), and a spatial distribution of CBFs was obtained (Figure 4C). In the CBF map, significant local variance was observed in the beating frequencies within the same organoid. The beating frequencies ranged between 5 and 10 Hz (mean: 7, median: 7, standard deviation: 1.8) (Figure 4C) at room temperature (23–25°C), which is a typical result for healthy airway cells according to previous studies [34], [35]. Based on CBF maps, other organoids (#2 and #3 in Figure 4A) also exhibited similar intra-ciliary CBF variations (Figs. 4D, 4E), as shown in the histograms (Figure 4F). This spatial

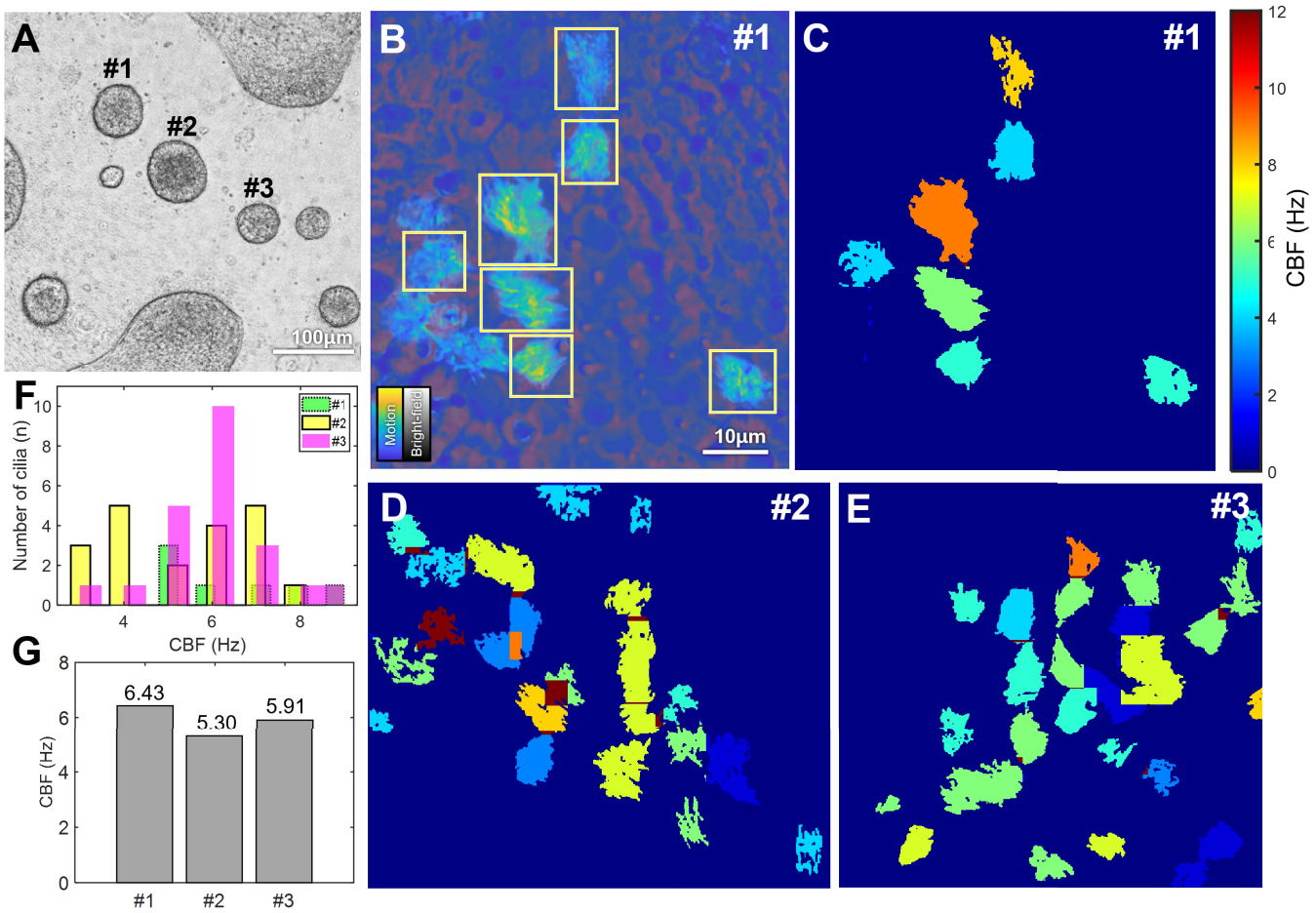

Fig. 4. Proposed method determines spatial distribution of CBF in a video. (A) Bright-field image of the organoids from ciliopathy-free progenitor cells in a culture dish. (B) Overlaid (motion-contrast + original) image obtained from organoid #1 in (A). (C) The corresponding CBF map. (D) and (E) display additional spatial CBF maps of neighboring organoids, #2 and #3 in (A). (F) Histogram depicting that CBFs within the organoid exhibits wide variance. (G) CBF variance between organoids is reduced in comparison to single-point measurements.

heterogeneity in the collective dynamics of ciliary beating in the epithelium has been observed with multiple CBF imaging technologies [20], [21], [36]. Further, it could be crucial for effective mucociliary clearance in airways [37], [38]. However, for the three organoids (#1–3), the respective CBF maps had average values of 6.43, 5.30, and 5.91 Hz (Figure 4G), showing minor ciliary variations between the organoids.

E. Temperature Dependence of CBF

Both *in vitro* and *in vivo* experiments have demonstrated that CBF exhibits variation with temperature [21], [39]–[41]. We verified this observation via longitudinal measurements of five ciliated cells in two organoids. In the organoid (Figure 5A) subject to temperature variations (23–32 °C), the movement of cilia on the organoids and CBF increased swiftly with temperature (Fig. 5B, Supplementary Video 2), as expected [21], [39]–[41]. For all five cells from the two organoids, the mean CBF increased linearly from 5.63 to 9.72 Hz, with a corresponding increase in variance and mean values (Figure 5C). When fit to a line, the CBF values exhibited a slope of 0.5 Hz/°C.

F. Uncoordinated Ciliary Motion in a Gene-Edited Organoid Model of a Respiratory Disorder

DAAF4 is one of the assembly factors for dynein in cilia and is known as one of the PCD-causing genes [42]. Using CRISPR/Cas9, we introduced indels in normal lung airway organoids to model a DAAF4 mutation found in a Korean PCD family (unpublished), which is a truncation mutation at the eighth of nine exons (c.1016dupA p.Asn339fs). Sanger sequencing of the edited organoids showed that the indels was generated 3 bp next to the protospacer adjacent motif (PAM) site, as expected, and the editing efficiency was roughly 10 % (Supplementary Figure). This low-yield guide RNA was chosen to evaluate the ability of our method under conditions where selection bias could easily intervene.

Figs. 6A and 6B shows a bright-field image of the gene-edited human epithelial lung airway organoid overlaid on its motion-contrast image. Interestingly, a large portion of cilia in the gene-edited organoid exhibited non-oscillatory correlation profiles with peaks less than 0.6 (Figure 6C). These low coefficients could be due to the uncoordinated ciliary motion of the cells, which was identified from optical flows (insets in Figure 6C) of the gene-edited and control cilia images, where the gene-edited cilia had unpolarized (red arrows in

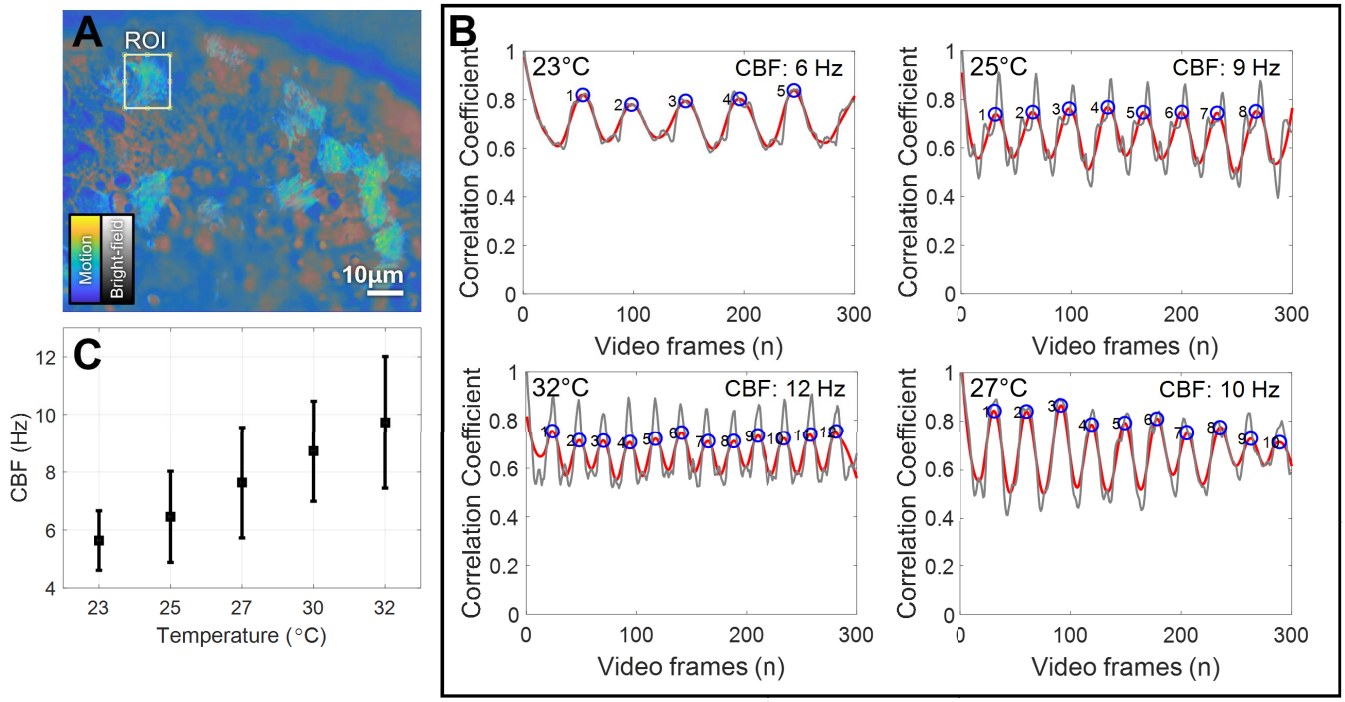

Fig. 5. Application of the devised method in analyzing CBF temperature dependence. (A) Motion-contrast image overlaid on a greyscale micrograph of a human airway epithelial organoid. (B) Change in CBF correlations with temperature (23-32°C). Measurements were obtained from within an ROI [yellow box in (A)]. (C) Dependence of the CBF on temperature for different ROIs from two organoids (sample size, $n = 5$).

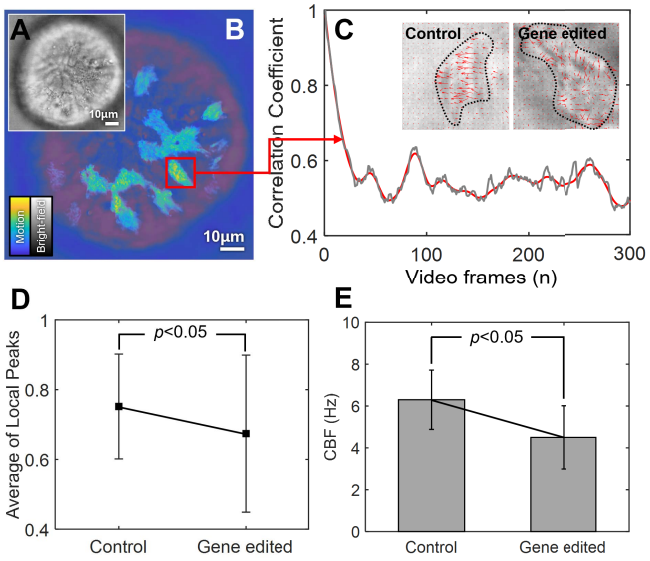

Fig. 6. CBF measurement in a human airway organoid model for primary ciliary dyskinesia (PCD). (A) Microscope image of a human airway organoid with the DAAF4 truncated mutation introduced by CRISPR/Cas9. (B) Overlaid (motion-contrast + original) image with an ROI (red box). (C) Correlation profile corresponding to the ROI. Insets are optical flow vectors (red arrows in dotted area) of cilia in the un-edited (control) and gene-edited organoids. (D) Comparison of the correlation coefficients for the control ($n = 20$) and gene-edited ciliated cells ($n = 20$). (E) Comparison of CBFs between the control ($n = 8$) and gene-edited ($n = 8$) at room temperature.

dotted boundary) motion pattern (Supplementary Video 3) whereas the control had directed motion (Supplementary Video 4). The average of the local peaks of the coefficient waveform was measured from individual cilia ($n = 20$) in the three controls and three gene-edited organoids under the same temperature (24 °C). We note that the mutant cilia exhibited wider variance (0.448–0.899) in the average scores compared to the control cilia (0.602–0.902) as shown in Figure 6D. The mean values were 0.777 (control), and 0.671 (gene-edited). With a low correlation (<0.6), it can be difficult to obtain a significant CBF. However, for cilia ($n = 8$) with peak averages above 0.7 (threshold), the mean CBF (4.5 Hz) of the mutant cilia was significantly lower than that of the control (6.3 Hz) (Figure 6E, Supplementary Video 5). This finding illustrated that our method can quantitatively detect dysfunctional ciliary motion.

IV. Discussion

Airway ciliary beating is crucial for mucociliary clearance within the respiratory tract. Analyzing beating frequency is important for investigating lung biology and diagnosing pathological conditions associated with impaired ciliary motion. Earlier, CBF analysis methods were highly time-consuming and required extensive operator attention. The recent advent of high-speed digital cameras and the development of advanced computerized analysis algorithms have enabled simpler and faster CBF measurements *in vitro* and *ex vivo*.

However, the current techniques have posed a challenge for credible measurements. For example, Sisson-Ammons video analysis [16], a standardized assay currently available for CBF analysis, has several drawbacks. The conventional method can measure CBFs only on small ROIs and the choice of ROIs is highly subjective for users, which may induce a possible

selection bias during ciliary measurements. The effect may be even worse in samples with variable CBFs like gene-edited organoids. Moreover, CBF values estimated via the single-point-based FFT approach may be ambiguous due to the signal redundancy issue, as illustrated in Figure 2.

Meanwhile, the technique introduced in this paper offers significant improvements over the existing methods. The motion-contrast imaging provides discernable cilia against the background, which enables for users to locate the ROI without errors. Furthermore, the image-based correlation approach automatically determines an effective CBF for individual motile cilia in the user-selected area. This metric can characterize a broad distribution of frequencies with high sensitivity in the organoid. In addition, the correlation strategy used can be tolerable to the signal blurring induced by focal shifts since its measurements are based on the similarity of the image textures, which improves fidelity in the measurements.

In our study, the majority of cilia on the edited organoid models for PCD exhibited a much lower inter-frame correlation compared to the healthy control. The lack of correlation is indicative of abnormal ciliary motion. This could be due to the asynchronous beats and incomplete strokes often found in the cilia of patients with respiratory diseases [19], [43], which were experimentally identified by comparison of the optical flow vectors (insets in Fig. 6C). When complementing CBF, the directional flow vectors may also be a good indicator to characterize the physiological aspects of ciliary dysfunction in a visual way, given that the orchestra of ciliary movement is a more fundamental and functional characteristic of mucociliary clearance than any single parameter of ciliary movement. Although some cilia in the edited organoids showed coordinated beatings in motion, their CBFs at room temperature decreased significantly compared to CBFs in the control organoids (Figure 6E). Furthermore, a couple of motionless cilia were also observed in the gene-edited organoids. In this case, the CBFs (ideally 0) of the stationary cilia could be measured with the composite motion-contrast image including bright-field imaging.

The proposed method is independent to the microscope system and can be readily applied to all videos recorded from commercially available or laboratory-made high-resolution, high-speed reflectance microscopes used in clinic or for biomedical research. It may be incorporated into present clinical workflows for the testing of ciliary motility by brush biopsy and by ciliary culture. In this case, it may be necessary to upgrade microscope cameras to a high-speed ($>$100 fps) imaging device, but the actual analysis may be performed either by standalone software which analyzes previously captured high-speed videos, or as a plug-in to already-integrated microscopy capture and analysis solutions such as μManager [44]. Briefly, said software would prompt for ROIs, and then return CBF statistics alongside CBF and optical flow vector maps.

A freehand version of our CBF analysis software is currently being developed. It will be integrated into touchscreen displays, which will enable users to quickly measure the CBFs in any hand-drawn ROIs using touchscreen pens or bare fingers. This custom touch solution would be beneficial for physicians as it would enable analysis of the video images of a patient's upper airway captured by bronchoscopes, tracheal endoscopes, or nasal endoscopes equipped with cellular resolution endomicroscopy technologies [45]–[47].

V. Conclusion

In summary, we presented an improved video microscopy method for the analysis of the ciliary beat patterns. With the help of this approach, the CBF values of individual multiciliated cells on the human airway organoid were assessed with a high level of accuracy. We believe that the method can be utilized for objective diagnosis of partial ciliopathies and in-depth automated analyses of ciliopathy characteristics.

References

[1] R. Jain *et al.*, "Temporal relationship between primary and motile ciliogenesis in airway epithelial cells," *Amer. J. Respiratory Cell Mol. Biol.*, vol. 43, no. 6, pp. 731–739, Dec. 2010.

[2] E. W. Olstad *et al.*, "Ciliary beating compartmentalizes cerebrospinal fluid flow in the brain and regulates ventricular development," *Curr. Biol.*, vol. 29, no. 2, pp. 229–241, Jan. 2019.

[3] R. A. Lyons, E. Saridogan, and O. Djahanbakhch, "The reproductive significance of human fallopian tube cilia," *Human Reproduction Update*, vol. 12, no. 4, pp. 363–372, Aug. 2006.

[4] J. Elgeti and G. Gompper, "Emergence of metachronal waves in cilia arrays," *Proc. Nat. Acad. Sci. USA*, vol. 110, no. 12, pp. 4470–4475, Mar. 2013.

[5] X. M. Bustamante-Marin and L. E. Ostrowski, "Cilia and mucociliary clearance," *Cold Spring Harbor Perspect. Biol.*, vol. 9, no. 4, Apr. 2017, Art. no. a028241.

[6] M. Fliegauf, T. Benzing, and H. Omran, "When cilia go bad: Cilia defects and ciliopathies," *Nature Rev. Mol. Cell Biol.*, vol. 8, no. 11, pp. 880–893, Nov. 2007.

[7] A. Bush *et al.*, "Primary ciliary dyskinesia: Diagnosis and standards of care," *Eur. Respiratory J.*, vol. 12, no. 4, pp. 982–988, Oct. 1998.

[8] M. W. Leigh, A. Horani, B. Kinghorn, M. G. O'Connor, M. A. Zariwala, and M. R. Knowles, "Primary ciliary dyskinesia (PCD): A genetic disorder of motile cilia," *Transl. Sci. Rare Diseases*, vol. 4, nos. 1–2, pp. 51–75, Jul. 2019.

[9] A. Yaghi and M. Dolovich, "Airway epithelial cell cilia and obstructive lung disease," *Cells*, vol. 5, no. 4, p. 40, Nov. 2016.

[10] A. E. Tilley, M. S. Walters, R. Shaykhiev, and R. G. Crystal, "Cilia dysfunction in lung disease," *Annu. Rev. Physiol.*, vol. 77, no. 1, pp. 379–406, Feb. 2015.

[11] B. Thomas, A. Rutman, and C. O'Callaghan, "Disrupted ciliated epithelium shows slower ciliary beat frequency and increased dyskinesia," *Eur. Respiratory J.*, vol. 34, no. 2, pp. 401–404, Aug. 2009.

[12] T. Dalhamn, "Ciliary motility studies," *Arch. Internal Med.*, vol. 126, no. 3, p. 424, Sep. 1970.

[13] D. A. Selwyn, A. Gyi, J. H. Raphael, A. Key, and J. A. Langton, "A perfusion system for *in vitro* measurement of human cilia beat frequency," *Brit. J. Anaesthesia*, vol. 76, no. 1, pp. 111–115, Jan. 1996.

[14] M. J. Sanderson and E. R. Dirksen, "A versatile and quantitative computer-assisted photoelectronic technique used for the analysis of ciliary beat cycles," *Cell Motility*, vol. 5, no. 4, pp. 267–292, 1985.

[15] T. Dalhamn and R. Rylander, "Frequency of ciliary beat measured with a photo-sensitive cell," *Nature*, vol. 196, no. 4854, pp. 592–593, Nov. 1962.

[16] J. H. Sisson, J. A. Stoner, B. A. Ammons, and T. A. Wyatt, "All-digital image capture and whole-field analysis of ciliary beat frequency," *J. Microsc.*, vol. 211, no. 2, pp. 103–111, Aug. 2003.

[17] S. Dimova, F. Maes, M. E. Brewster, M. Jorissen, M. Noppe, and P. Augustijns, "High-speed digital imaging method for ciliary beat frequency measurement," *J. Pharmacy Pharmacol.*, vol. 57, no. 4, pp. 521–526, Feb. 2010.

[18] C. M. Smith *et al.*, "CiliaFA: A research tool for automated, high-throughput measurement of ciliary beat frequency using freely available software," *Cilia*, vol. 1, no. 1, p. 14, Dec. 2012.

[19] J. Raidt *et al.*, "Ciliary beat pattern and frequency in genetic variants of primary ciliary dyskinesia," *Eur. Respiratory J.*, vol. 44, no. 6, pp. 1579–1588, Dec. 2014.

[20] L. Feriani *et al.*, "Assessing the collective dynamics of motile cilia in cultures of human airway cells by multiscale DDM," *Biophys. J.*, vol. 113, no. 1, pp. 109–119, Jul. 2017.
[21] Y. He, J. C. Jing, Y. Qu, B. J. Wong, and Z. Chen, "Spatial mapping of tracheal ciliary beat frequency using real time phase-resolved Doppler spectrally encoded interferometric microscopy," *ACS Photon.*, vol. 7, no. 1, pp. 128–134, Jan. 2020.
[22] G. M. Solomon *et al.*, "Assessment of ciliary phenotype in primary ciliary dyskinesia by micro-optical coherence tomography," *JCI Insight*, vol. 2, no. 5, Mar. 2017, Art. no. e91702.
[23] G. Rossi, A. Manfrin, and M. P. Lutolf, "Progress and potential in organoid research," *Nature Rev. Genet.*, vol. 19, no. 11, pp. 671–687, Nov. 2018.
[24] F. Schutgens and H. Clevers, "Human organoids: Tools for understanding biology and treating diseases," *Annu. Rev. Pathol., Mech. Disease*, vol. 15, no. 1, pp. 211–234, Jan. 2020.
[25] C. E. Barkauskas, M.-I. Chung, B. Fioret, X. Gao, H. Katsura, and B. L. M. Hogan, "Lung organoids: Current uses and future promise," *Development*, vol. 144, no. 6, pp. 986–997, Mar. 2017.
[26] N. Sachs *et al.*, "Long-term expanding human airway organoids for disease modeling," *EMBO J.*, vol. 38, no. 4, Feb. 2019, Art. no. e100300.
[27] Q. Tan, K. M. Choi, D. Sicard, and D. J. Tschumperlin, "Human airway organoid engineering as a step toward lung regeneration and disease modeling," *Biomaterials*, vol. 113, pp. 118–132, Jan. 2017.
[28] B. Artegiani *et al.*, "Fast and efficient generation of knock-in human organoids using homology-independent CRISPR-Cas9 precision genome editing," *Nat. Cell Biol.*, vol. 22, no. 3, pp. 321–331, Mar. 2020.
[29] E. Driehuis and H. Clevers, "CRISPR/Cas 9 genome editing and its applications in organoids," *Amer. J. Physiol.-Gastrointestinal Liver Physiol.*, vol. 312, no. 3, pp. G257–G265, Mar. 2017.
[30] X. Ding, T. Seebeck, Y. Feng, Y. Jiang, G. D. Davis, and F. Chen, "Improving CRISPR-Cas9 genome editing efficiency by fusion with chromatin-modulating peptides," *CRISPR J.*, vol. 2, no. 1, pp. 51–63, Feb. 2019.
[31] X.-H. Zhang, L. Y. Tee, X.-G. Wang, Q.-S. Huang, and S.-H. Yang, "Off-target effects in CRISPR/Cas9-mediated genome engineering," *Mol. Therapy Nucleic Acids*, vol. 4, p. e264, Jan. 2015.
[32] N. E. Sanjana, O. Shalem, and F. Zhang, "Improved vectors and genome-wide libraries for CRISPR screening," *Nature Methods*, vol. 11, no. 8, pp. 783–784, Aug. 2014.
[33] S. Yousefi, Z. Zhi, and R. K. Wang, "Eigendecomposition-based clutter filtering technique for optical microangiography," *IEEE Trans. Biomed. Eng.*, vol. 58, no. 8, pp. 2316–2323, Aug. 2011.
[34] Z. Sutto, G. E. Conner, and M. Salathe, "Regulation of human airway ciliary beat frequency by intracellular pH: Human airway ciliary beat frequency and intracellular pH," *J. Physiol.*, vol. 560, no. 2, pp. 519–532, Oct. 2004.
[35] A. Oltean, A. J. Schaffer, P. V. Bayly, and S. L. Brody, "Quantifying ciliary dynamics during assembly reveals stepwise waveform maturation in airway cells," *Amer. J. Respiratory Cell Mol. Biol.*, vol. 59, no. 4, pp. 511–522, Oct. 2018.
[36] M. Chioccioli, L. Feriani, J. Kotar, P. E. Bratcher, and P. Cicuta, "Phenotyping ciliary dynamics and coordination in response to CFTR-modulators in cystic fibrosis respiratory epithelial cells," *Nature Commun.*, vol. 10, no. 1, p. 1763, Dec. 2019.
[37] S. Dey, G. Massiera, and E. Pitard, "Role of spatial heterogeneity in the collective dynamics of cilia beating in a minimal one-dimensional model," *Phys. Rev. E, Stat. Phys. Plasmas Fluids Relat. Interdiscip. Top.*, vol. 97, no. 1, Jan. 2018, Art. no. 012403.
[38] G. R. R.-S. Juan, A. J. T. M. Mathijssen, M. He, L. Jan, W. Marshall, and M. Prakash, "Multi-scale spatial heterogeneity enhances particle clearance in airway ciliary arrays," *Nature Phys.*, vol. 16, no. 9, pp. 958–964, Sep. 2020.
[39] W. Nikolaizik, J. Hahn, M. Bauck, and S. Weber, "Comparison of ciliary beat frequencies at different temperatures in young adults," *ERJ Open Res.*, vol. 6, no. 4, Oct. 2020, Art. no. 00477.
[40] A. B. Christopher *et al.*, "The effects of temperature and anesthetic agents on ciliary function in murine respiratory epithelia," *Frontiers Pediatrics*, vol. 2, p. 111, Oct. 2014.
[41] Y. He, Y. Qu, J. C. Jing, and Z. Chen, "Characterization of oviduct ciliary beat frequency using real time phase resolved Doppler spectrally encoded interferometric microscopy," *Biomed. Opt. Exp.*, vol. 10, no. 11, p. 5650, Nov. 2019.
[42] A. Tarkar *et al.*, "DYX1C1 is required for axonemal dynein assembly and ciliary motility," *Nat. Genet.*, vol. 45, no. 9, pp. 995–1003, Sep. 2013.
[43] S. P. Quinn, M. J. Zahid, J. R. Durkin, R. J. Francis, C. W. Lo, and S. C. Chennubhotla, "Automated identification of abnormal respiratory ciliary motion in nasal biopsies," *Sci. Transl. Med.*, vol. 7, no. 299, Aug. 2015, Art. no. 299ra124.
[44] A. Edelstein, N. Amodaj, K. Hoover, R. Vale, and N. Stuurman, "Computer control of microscopes using μManager," *Current Protocols Mol. Biol.*, vol. 92, no. 1, pp. 1–17, Oct. 2010.
[45] L. Vanherp *et al.*, "Bronchoscopic fibered confocal fluorescence microscopy for longitudinal *in vivo* assessment of pulmonary fungal infections in free-breathing mice," *Sci. Rep.*, vol. 8, no. 1, p. 3009, Dec. 2018.
[46] J. R. Perez, N. Ybarra, F. Chagnon, O. Lesur, J. Seuntjens, and I. E. Naqa, "Fluorescence endomicroscopy imaging of mesenchymal stem cells in the rat lung," *Current Protocols Stem Cell Biol.*, vol. 45, no. 1, p. e52, May 2018.
[47] J. K. Kim *et al.*, "*In vivo* imaging of tracheal epithelial cells in mice during airway regeneration," *Amer. J. Respiratory Cell Mol. Biol.*, vol. 47, no. 6, pp. 864–868, Dec. 2012.